Quantum transport of 2D Weyl VSi_2N_4-based magnetic tunnel junction: a $k \cdot p$-NEGF study

Guohui Zhan[1,2], Kun Luo[1], Ruoran Jia[3], Christopher Yang[3*], Zhenhua Wu[1,2*]
[1] Institute of Microelectronics, Chinese Academy of Sciences, Beijing 100029, China.
[2] University of Chinese Academy of Sciences, Beijing 100049, China. Email: wuzhenhua@ime.ac.cn
[3] ChangXin Memory Technologies, Inc. Hefei, China. Email: Christopher.Yang@cxmt.com

***Abstract*—We present a systematical simulation on the room temperature strained VSi_2N_4-based magnetic tunnel junctions (MTJs). Based on $k \cdot p$-NEGF quantum transport modeling, the HSE06 band structure around the Fermi level was fitted by Weyl-like Hamiltonian, due to the fully spin-polarized Weyl band feature, a giant TMR ratio and perfect spin injection efficiency (SIE) were theoretically predicted in the MTJs devices. In addition, the current through the MTJs would increase when an elastic electron-phonon (e-ph) coupling effect is included in the quantum transport.**

I. Introduction

MTJs have attracted wide interest for their successful application, such as magnetoresistive random access memory devices (MRAM). To the demand of devices scaling down, two-dimensional (2D) materials-based MTJs provide an excellent and promising platform to explore next-generation spintronics devices. Recently, 2D $MoSi_2N_4$ material was successfully grown by chemical vapor deposition (CVD) method [1], it has been reported that some of MX_2Z_4 (M = Mo, W, V; X = Si, Ge; Z = N, P, As.) family may hold the Curie temperature (T_C) near to room temperature [2], and Wu *et. al.* have theoretically predicted that VSi_2N_4-based MTJs exhibit giant tunnel magnetoresistance (TMR) [3], they may be good candidates for designing scaled MTJ devices. However, some previous results were calculated based on regular PBE functional, more accurate HSE06 band structures showed that monolayer VSi_2N_4 is a magnetic semiconductor rather than a mental [4], therefore an accurate and comprehensive HSE06 level quantum transport results are lacking. In this work, by constructing the whole VSi_2N_4-based MTJs device Hamiltonian based on accurate $k \cdot p$ bulk band, spin-resolved quantum transport properties would be simulated by in-house code based on non-equilibrium green function (NEGF) formalism. It's obvious that the $k \cdot p$-NEGF method may effectively reduce the computational cost, and simply consider more physical effects, such as e-ph scattering, and vacancies. We found that the band structure around the fermi level of biaxial strained-VSi_2N_4 exhibits typical 2D Weyl behavior. Our $k \cdot p$-NEGF quantum transport results showed that a giant TMR values would be achieved in this lateral VSi_2N_4-based MTJs device, which is consistent with previously reported DFT-NEGF results [3], [4].

II. Computational Methods

The electronic properties of MTJs materials with HSE06 level are performed by Synopsys QuantumATK-2022 [5]. The recursive Greens function (RGF) algorithm was applied for calculating the Greens function of the system. The retarded Green's function is obtained from:

$$G = [EI - H - \Sigma_L - \Sigma_R - \Sigma_s]^{-1} \tag{1}$$

where Σ_L, Σ_R and Σ_s are self-energies of left/right and center scattering region. The current at any terminal i of devices can be calculated from:

$$I_i = \frac{e}{h}\int_{-\infty}^{+\infty}(\mathrm{Trace}[\Sigma_i^{in}A] - \mathrm{Trace}[\Gamma_i G^n])dE. \tag{2}$$

where A, G^n is spectrum and correlation function. $\Sigma_i^{in} = \Gamma_i f_i$. If the scattering process is elastic, $\Sigma_s^{in} = D_0 G^n(E), \Sigma_s(E) = D_0 G(E)$, where D_0 is the e-ph coupling strength [6]. In our work, the charge correction from Poisson equation had been neglected due to the low field condition.

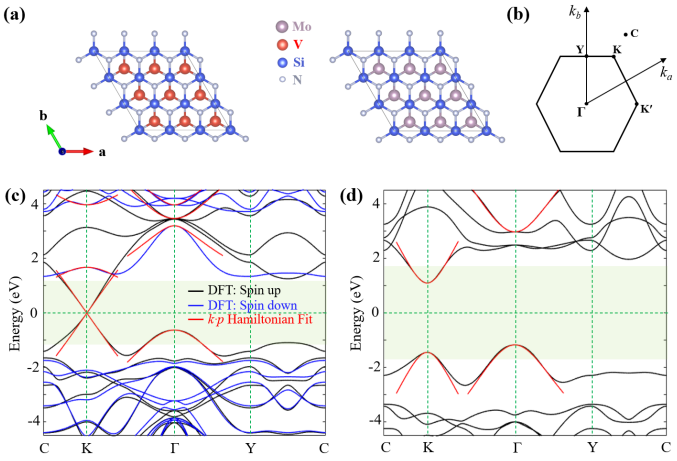

Fig. 1. (a) Top view of crystal VSi_2N_4 and $MoSi_2N_4$; (b) High-symmetry points in Brillouin zone; (c) and (d) Band structure of strained VSi_2N_4 and $MoSi_2N_4$ with HSE06 level, where black, blue and red lines denote the spin up, down and the fitting band with $k \cdot p$ Hamiltonian, respectively. The shaded areas around Fermi energy indicate that the $k \cdot p$ band fits well.

III. Results and Discussion

Fig. 1(a) shows the crystal structure of the monolayer VSi_2N_4 and $MoSi_2N_4$. The nonmagnetic structure is described by the point group D_{3h}. The magnetic moment of the V atom is about 0.9 μ_B. Some Refs reported that VSi_2N_4 is magnetic metal based on PBE functional [1], [3], [7], but reliable HSE06

results showed that VSi_2N_4 is a magnetic semiconductor. Moreover, after applying a slight 1.965% biaxial strain [4], the gap is closed and forms a fully spin-polarized Weyl cone around the Fermi energy, as shown in Fig. 1(c). In addition, $MoSi_2N_4$ is an insulator with around 2.2 eV band gap (Fig. 1(d)). Because the small spin-orbit coupling effect is neglected in our work. Similar to Ref. [8], the effective Hamiltonian model around $K(K')$ have the form based on group theory:

$$H(k_x, k_y) = v_f(\tau k_x \sigma_x + k_y \sigma_y) + \frac{\Delta}{2}\sigma_z + E_0\sigma_0 \qquad (3)$$

where v_f denote the fermi velocity around the Weyl cone, $\tau = \pm 1$ for the K or K' point. Δ denote the band gap, E_0 is constant term. Because of similar symmetry constraints, the band structure around Γ point has a similar Hamiltonian form. All $k \cdot p$ Hamiltonian fitting parameters are listed in Table I.

TABLE I
THE $k \cdot p$ FITTING PARAMETERS OF VSi_2N_4 AND $MoSi_2N_4$

	K/K'			Γ		
	v_f	Δ	E_0	v_f	Δ	E_0
VSi_2N_4 up	3.2	0.0	-0.0119	3.45	4.086	1.408
VSi_2N_4 down	2.0	2.289	2.8065	2.0	0.766	3.565
$MoSi_2N_4$	5.0	2.538	-0.179	4.5	4.134	0.894

[a] Units, v_f: eV*Å, Δ: eV, E_0: eV.

Fig. 2(a) shows the lateral MTJ device, where the insulated $MoSi_2N_4$ is viewed as a barrier due to the similar crystal structure. The two materials would match perfectly to form a heterojunction. The VSi_2N_4 on the left region is viewed as a fixed layer, while the VSi_2N_4 on the right region is viewed as a free layer where the magnetic moment can be flipped. A simple band alignment of VSi_2N_4 and $MoSi_2N_4$ along y-direction is depicted in Fig. 2(b). For numerical calculation based on finite difference method, we first discretize the $k \cdot p$ Hamiltonian (like Eq. (3)) around $K/K', \Gamma$ points in the real space by converting $k_y = -i\partial/\partial y$. The grid space is 1 Å, and the length of the device are set to 4.5 nm: the fixed ('L'), insulator ('C'), and free ('R') region are 1.5nm, thus the Hamiltonian matrix of the device can be obtained

$$\begin{pmatrix} HL_{00} & HL_{01} & & & & & \\ HL_{10} & HL_{00} & HL_{01} & & & & \\ & \cdots & \cdots & \cdots & & & \\ & & HC_{10} & HC_{00} & HC_{01} & & \\ & & & \cdots & \cdots & \cdots & \\ & & & & HR_{10} & HR_{00} & HR_{01} \\ & & & & & HR_{10} & HR_{00} \end{pmatrix}$$

where H_{00} and H_{01} represents onsite term and the nearest neighbor term along y-direction . To simplify the problem, the block Hamiltonian H_{00} and H_{01} for the contact region of the VSi_2N_4 and $MoSi_2N_4$ is set to average interactions $(HL + HC)/2, (HC + HR)/2$. Then the Green function of the whole device would be constructed, some key transport properties, such as transmission, and IV characteristics, can be calculated based on iterative Green's methods.

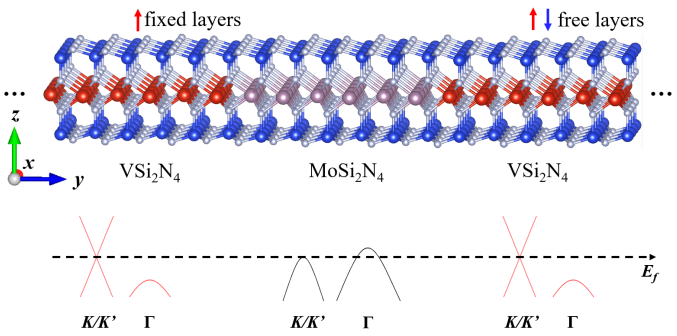

Fig. 2. (a) The device model of lateral VSi_2N_4-$MoSi_2N_4$-VSi_2N_4 MTJs, the transport direction along the y-axis. (b) The band alignment around K, Γ of MTJ device.

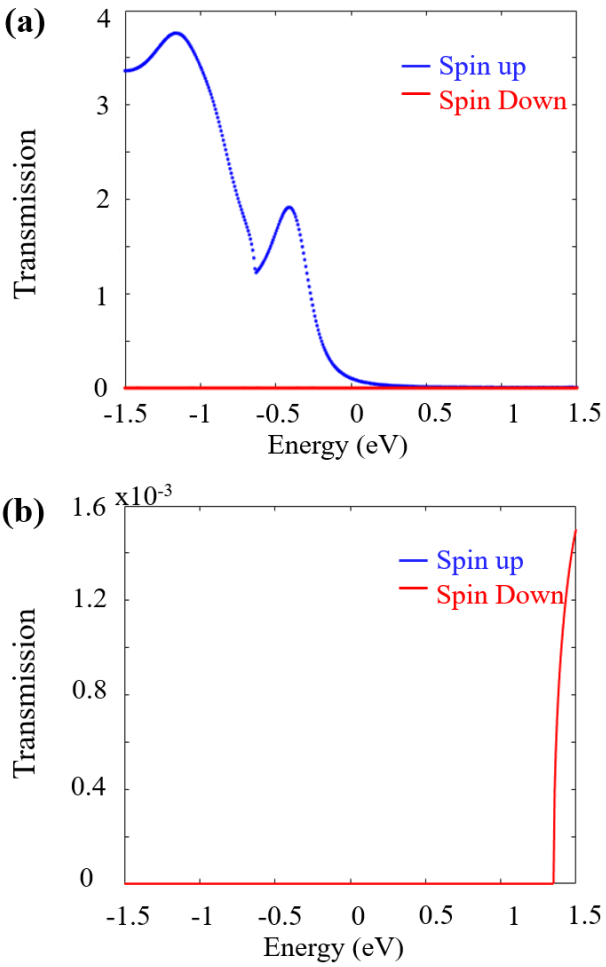

Fig. 3. The transmission spectrum of P (a) and AP (b) configuration of device, the blue and red represent the spin up and down channel.

For coherent transport, one can calculate the transmission from the Green's function, using the relation $T(E) = \mathrm{Trace}[\Gamma_L G \Gamma_R G^\dagger]$. As shown in Fig. 3, the transmission in parallel (P) configuration is larger than in anti-parallel (AP) configuration (almost zero), indicating a giant tunnel magnetoresistance, and the transmission of spin up channel is greater on spin down channel in P configuration, this is due to the large spin polarization around the Fermi level in Fig. 1(c). To obtain better insight into the physical picture, we also calculated the projected local density of states (PLDOS) in P and AP configuration (Fig. 4), For P configuration, there is a majority density of states for the spin-up channel, showing that the up channel is of low resistance. In contrast, there is no density of states near the Fermi energy the spin-down channel in left/right region, indicating that the spin-down channel is of high resistance. For AP configuration, the spin-up and spin-down have similar transmission probability.

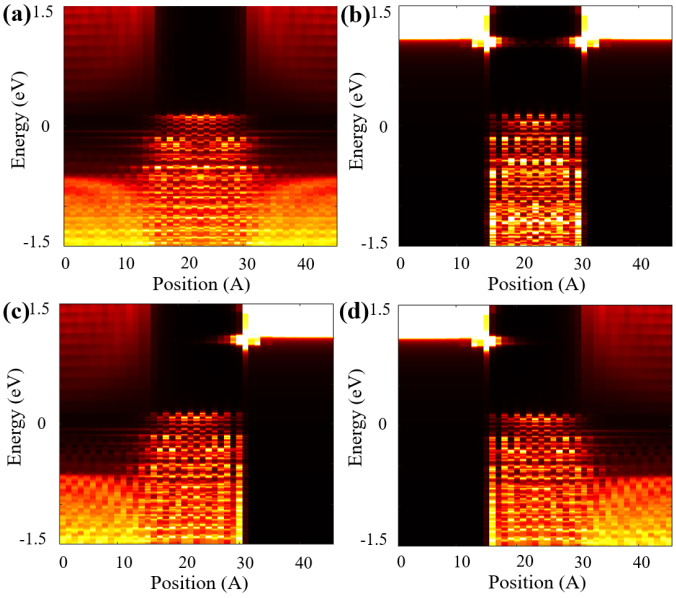

Fig. 4. The PLDOS in P (a-b) and AP (c-d) configuration under equilibrium states. (a,c) shows the spin-up and (b,d) shows spin-down channel.

Fig. 5 shows the IV characteristics under low bias in P and AP configuration. P configuration holds a larger current while almost zero current in AP configuration. The TMR ratio is defined as $\mathrm{TMR} = \frac{I_\mathrm{P} - I_\mathrm{AP}}{I_\mathrm{AP}}$, and the spin injection efficiency (SIE) is $\mathrm{SIE} = \frac{I_{up} - I_{down}}{I_{up} + I_{down}}$. It's found that there are about $10^{32}\%$ TMR values and perfect SIE values. Compared with the $10^{11}\%$ TMR of PBE calculated [3], the result of the HSE06 calculation is significantly improved. To be honest, the predicted TMR value is a bit exaggerated, much higher than the current experimental TMR. it's a very simple and ideal physical model that ignores many important realistic factors in experiments, but to some extent, it shows that this VSi_2N_4-based MTJ has a large TMR value.

To further take into account the noncoherent transport due to dephasing mechanisms, if the scattering process is elastic ($E \approx E \pm \hbar\omega$) [6], one introduces the dephasing

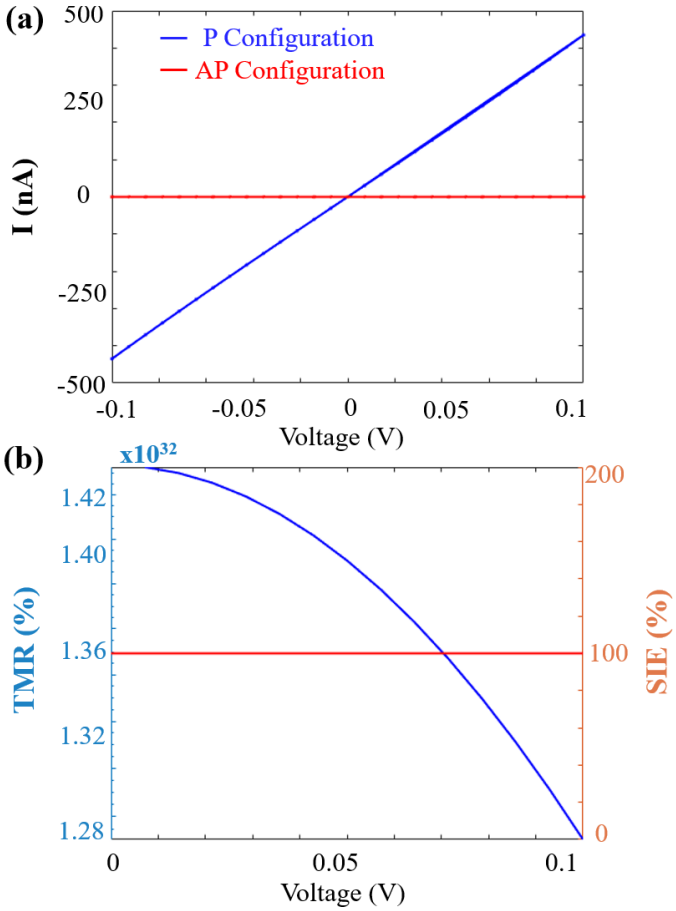

Fig. 5. (a) The I-V characteristics of MTJ devices, (b) TMR ratio and SIE as function of bias voltage.

matrix D_0, then $\Sigma_s^{in} = D_0 G^n(E), \Sigma_s(E) = D_0 G(E)$, under the noncoherent transport, the effective transmission is also defined as:

$$\bar{T}(E) = \frac{\mathrm{Trace}(\Sigma_i^{in} A) - \mathrm{Trace}(\Gamma_i G^n)}{f_L - f_R} \tag{4}$$

where f_L, f_R denote the Fermi-Dirac distribution of the left and right electrodes. As shown in Fig. 6, the applied voltage is set as 0.01 V, we found that when the coupling strength D_0 increases (from 0.00 eV^2 to 0.20 eV^2), the transmission, on the whole, shows a downward tendency, but the transmission increases abnormally near the Fermi energy. At last, we calculated the non-coherent current (Fig. 7) in P configuration with different dephasing strength D_0, it's found that the current increases significantly. Our results reveal that the current would be improved after the elastic e-ph scattering was added to the quantum transport.

IV. Conclusion

We theoretically studied the quantum transport of strained VSi_2N_4-based MTJs based on $k \cdot p$-NEGF formalism. A giant TMR ratio and perfect SIE value are theoretically predicted, and the current increases when an elastic electron-phonon

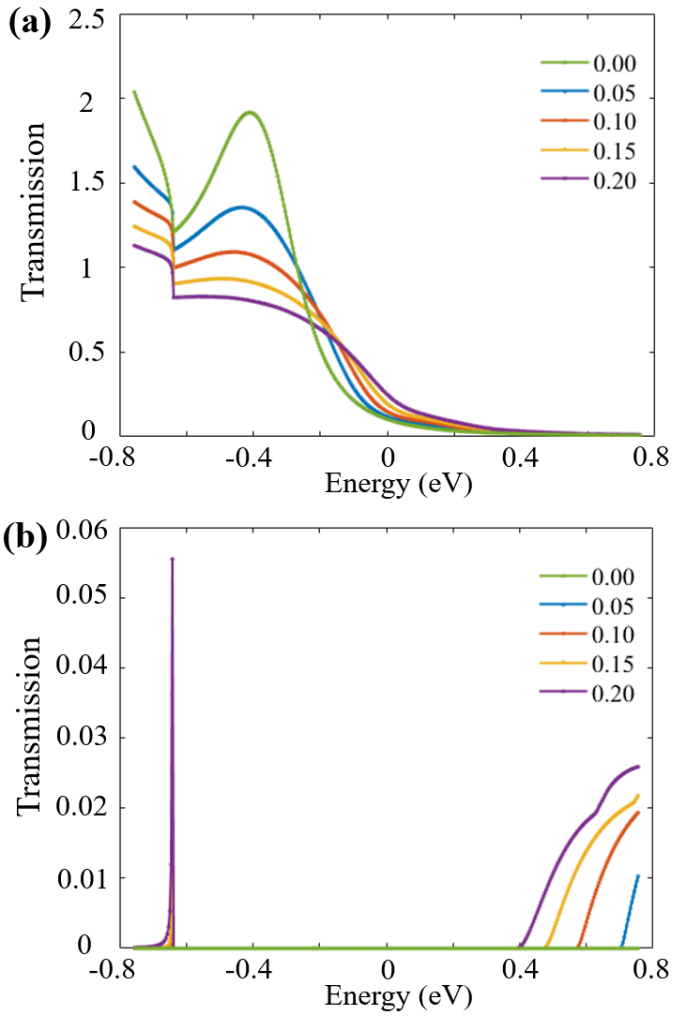

Fig. 6. The effective transmission in P (a) and AP (b) configuration with elastic dephasing, which the scattering strength $D_0 = 0.00 - 0.20$ eV^2. The bias voltage is 0.01 V.

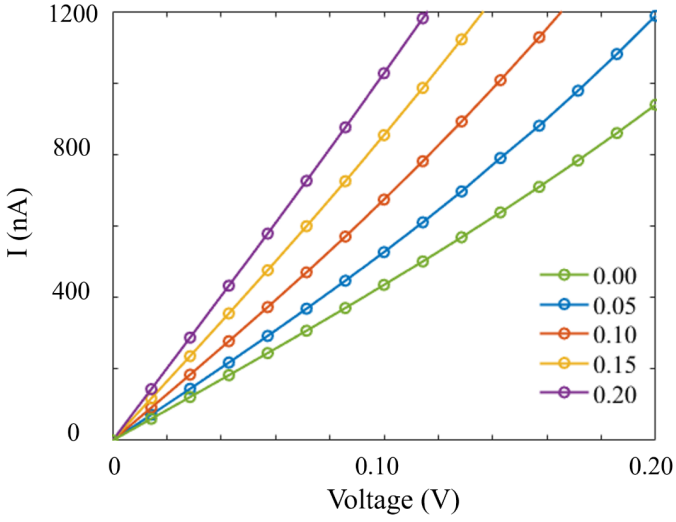

Fig. 7. The IV characteristics in P configuration with elastic dephasing, which the scattering strength $D_0 = 0.00 - 0.20$ eV^2.

scattering is accounted for. We believe that our results are helpful for the design and application of future two-dimensional spintronics devices.

ACKNOWLEDGMENT

This work is supported by the Ministry of Science and Technology (Grant No. 2021YFA1200502) and the National Natural Science Foundation of China (Grant No. 12174423).

REFERENCES

[1] Y.-L. Hong, Z. Liu, L. Wang, T. Zhou, W. Ma, C. Xu, S. Feng, L. Chen, M.-L. Chen, D.-M. Sun, X.-Q. Chen, H.-M. Cheng, and W. Ren, "Chemical vapor deposition of layered two-dimensional mosi2n4 materials," *Science*, vol. 369, no. 6504, pp. 670–674, 2020. [Online]. Available: https://doi.org/10.1126/science.abb7023

[2] L. Wang, Y. Shi, M. Liu, A. Zhang, Y.-L. Hong, R. Li, Q. Gao, M. Chen, W. Ren, H.-M. Cheng, Y. Li, and X.-Q. Chen, "Intercalated architecture of ma2z4 family layered van der waals materials with emerging topological, magnetic and superconducting properties," *Nature communications*, vol. 12, no. 1, pp. 1–10, 2021. [Online]. Available: https://www.nature.com/articles/s41467-021-22324-8

[3] Q. Wu and L. K. Ang, "Giant tunneling magnetoresistance in atomically thin vsi2n4/mosi2n4/vsi2n4 magnetic tunnel junction," *Applied Physics Letters*, vol. 120, no. 2, p. 022401, 2022. [Online]. Available: https://doi.org/10.1063/5.0075046

[4] G. Zhan, Z. Yang, K. Luo, S. Zhang, and Z. Wu, "Large magnetoresistance and perfect spin-injection efficiency in two-dimensional strained vsi_2n_4-based room-temperature magnetic-tunnel-junction devices," *Phys. Rev. Appl.*, vol. 19, p. 014020, Jan 2023. [Online]. Available: https://link.aps.org/doi/10.1103/PhysRevApplied.19.014020

[5] S. Smidstrup, T. Markussen, P. Vancraeyveld, J. Wellendorff, J. Schneider, T. Gunst, B. Verstichel, D. Stradi, P. A. Khomyakov, U. G. Vej-Hansen, M.-E. Lee, S. T. Chill, F. Rasmussen, G. Penazzi, F. Corsetti, A. Ojanper, K. Jensen, M. L. N. Palsgaard, U. Martinez, A. Blom, M. Brandbyge, and K. Stokbro, "Quantumatk: An integrated platform of electronic and atomic-scale modelling tools," *J. Phys: Condens. Matter*, vol. 32, p. 015901, 2020.

[6] S. Datta, *Quantum transport: atom to transistor*. Cambridge university press, 2005.

[7] M. R. K. Akanda and R. K. Lake, "Magnetic properties of nbsi2n4, vsi2n4, and vsi2p4 monolayers," *Applied Physics Letters*, vol. 119, no. 5, p. 052402, 2021. [Online]. Available: https://doi.org/10.1063/5.0055878

[8] D. Xiao, G.-B. Liu, W. Feng, X. Xu, and W. Yao, "Coupled spin and valley physics in monolayers of mos_2 and other group-vi dichalcogenides," *Phys. Rev. Lett.*, vol. 108, p. 196802, May 2012. [Online]. Available: https://link.aps.org/doi/10.1103/PhysRevLett.108.196802